

METHODOLOGY FOR DESIGN OF ACTIVE CONTROLS  
FOR V/STOL AIRCRAFT

George Meyer and Luigi Cicolani  
NASA Ames Research Center

ABSTRACT

An effort is underway at the Ames Research Center to develop techniques for the design of integrated, fully automatic flight control systems for powered lift STOL and VTOL aircraft. The paper describes the structure of the control system which has been developed to deal with the strong nonlinearities inherent in this class of aircraft; to admit automatic coupling with the advanced ATC requiring accurate execution of complex trajectories; and to admit a variety of active control tasks. The specific case being considered is the Augmentor Wing Research Aircraft.

INTRODUCTION

NASA through its STOL and VTOL research programs is investing substantial resources in developing powered lift technology. In all cases, the wide range of lift coefficient required to cover all flight conditions between cruise and landing is achieved by in-flight modification of aircraft configuration. These modifications result in drastic changes in control characteristics of the aircraft, and, particularly in the high-lift transition and landing configurations, the aircraft response to control inputs is very nonlinear. Moreover, the presence of powered and direct lift generators increases the total number of controls available to the pilot who must continually make decisions on control techniques. Finally, the coming short-haul transportation system will be required to satisfy stringent environmental constraints which will necessitate accurate execution of complex trajectories. Accurate, unaided manual tracking of complex trajectories by manipulating a large set of interacting controls of an aircraft whose control characteristics are non-linear and rapidly changing represents an unacceptably high pilot work load. Active control technology has the potential to provide a means for reducing the pilot work load to an acceptable level by integrating control functions in such a way as to generate desirable handling qualities without reduction in the performance of the aircraft as an element of the advanced civil air transportation system. The advantages of active control technology are potentially even more substantial in military applications of STOL and VTOL aircraft. Both the Advanced Military STOL and the Sea Control Fighter VTOL must utilize the maneuvering capacity of the basic aircraft to the fullest. The tracking of complex penetration trajectories must be sufficiently accurate for proper execution of mission, and the pilot work load associated with flying must not adversely affect his ability to perform other tasks. Again, the maneuverability, accuracy, and level of pilot work load can be improved by means of active

control technology. At the present time, however, the practical problems of applying the technology to powered lift aircraft are not well understood. In order to provide the required data base, an applications-oriented program has been initiated at the Ames Research Center. The objectives of this program are to generate design guide lines and to provide flight test confirmation required for incorporation of active control technology into this class of aircraft. The present paper describes the progress made in one segment of this program, namely, the development of a methodology for the design of automatic trajectory control systems for powered lift aircraft.

#### THE AUGMENTOR WING RESEARCH AIRCRAFT

The specific case being used in the development and tests of the design methodology is the Augmentor Wing Research Aircraft. The aircraft is a de Havilland C-8A "Buffalo" modified according to the general arrangement shown in figure 1. The aircraft is powered by two turbofan engines. The relatively cold flow from the front fans is ducted through the wing and fuselage to the augmented jet flap, blown ailerons, and fuselage boundary layer control systems. The hot gas flows through two pairs of nozzles which can be rotated in flight to provide vectoring of the hot thrust through a  $98^\circ$  range. The hot and cold thrusts are nonlinear functions of the throttle setting. The nozzle servos move the nozzles in unison in response to a single nozzle angle command. The system is quite fast, being limited to  $90^\circ/\text{sec.}$ . The throttle-to-thrust control system is relatively slow with a bandwidth of approximately  $1 \text{ (rad./sec.)}$ .

The cold flow has a pronounced effect on the lift and drag polars of the aircraft. For example, figure 2 shows the wing-body polars for two flap settings. The independent variables in the plots are the aircraft angle of attack,  $\alpha$ , and the cold thrust coefficient  $C_J = T_c/QS_w$ , where the cold thrust  $T_c$  is a nonlinear function of throttle, and density and temperature of the air;  $Q$  is the dynamic pressure, and  $S_w$  is the wing area. Of particular significance for the design of flight path control systems is the large variation in the basic aerodynamic characteristics of the aircraft.

Certainly, there is a large change between the cruise configuration (flap =  $4.5^\circ$ ) and the landing configuration (flap =  $65^\circ$ ). But present indications are that the nonlinearity is significant even over a much smaller region. For example, figure 3 shows the total lift and drag coefficients, including the effects of the hot thrust for the case of constant flap, throttle and speed which corresponds to a typical landing configuration with angle of attack and nozzle angle  $\nu$  in the active control mode. Point  $A_1$  in the figure represents equilibrium flight along the  $-7.5^\circ$  glide slope. Point  $A_2$  represents level flight. Also shown are the derivatives of the total force coefficient at these two points. As the aircraft is maneuvered from point  $A_1$  to point  $A_2$  the changes in these derivatives may adversely affect closed loop dynamics. But of greater concern is that if the maneuver is performed by means of a feed-forward command based on the linear model at point  $A_1$ , then the aircraft will be out of trim at  $A_2$  by  $\Delta C_L / C_L = 4.7\%$ . Because of bandwidth limitations imposed on the altitude control loop ( $\omega_n \leq 0.5 \text{ rad./sec.}$ ) by unsteady aerodynamics, the error in trim results in an altitude error  $\Delta h > 6 \text{ ft.}$  Similarly, transition from  $A_2$  to  $A_1$  will end up at  $A_{21}$ ; the corresponding error  $\Delta h > 16 \text{ ft.}$

Of course this hangoff error can be removed by means of an integrator, but the removal will be too slow for many maneuvers. Consequently, the transition between  $A_1$  and  $A_2$  must be considered to be nonlinear.

The design problem is further complicated by the presence of redundant controls. Thus, the two-dimensional total force coefficient  $C = (C_D, C_L)^T$  is a function, say  $C(F, T, \alpha, \nu)$ , of four variables, namely flap, throttle, angle of attack, and nozzle angle. For example, figure 4 shows the plot of  $C(F, T, \alpha, \nu) = C_0$ , where  $C_0$  corresponds to steady flight along  $-7.5^\circ$  glide slope. It may be noted that the plot is rather nonlinear. The problem is to be able to generate online optimum trim values of the controls  $(F, T, \alpha, \nu)$  for any admissible trim values of  $(C_D, C_L)$ .

#### DESIGN APPROACH

The approach is motivated by the following line of reasoning. Let equation (1) be the system state equation.

$$\dot{x} = f(x, u) \quad (1)$$

The control  $u$  is restricted to a set  $U$  which may depend on the state  $x$ . A trajectory  $(x_0(t), t \in T)$  is flyable if for all  $t \in T$ , there is a control  $u_0(t)$  such that

$$\dot{x}_0(t) = f(x_0(t), u_0(t)) \quad (2)$$

The trim problem is to find a control  $u_0$  satisfying (2), given that the trim trajectory is flyable. The solution will be an inverse of (1), namely a function  $(g, F)$ , which we call the trimmap, such that for all  $(\dot{x}, x) \in F$ ,

$$f(x, g(\dot{x}, x)) = \dot{x} \quad (3)$$

The corresponding trim control is given by

$$u_0 = g(\dot{x}_0, x_0) \quad (4)$$

Usually, trim refers to cases with constant  $u_0$ . Here  $u_0$  may vary with time. Note that when the controls are redundant, state equation (1) alone is not enough to define the trimmap  $(g, F)$ , and additional conditions must be introduced to resolve the redundancy.

The trim problem may be difficult to solve; but, evidently, its solution to required accuracy is the essential first step in the design of automatic flight path control systems. The next step usually taken is to design a control system based on perturbation models. Thus, given a flyable nominal trajectory  $(\dot{x}_0, x_0) \in F$  trimmed by  $u_0$  according to equation (4), the linear model (5) is obtained for the perturbations  $\delta x = x - x_0$  and  $\delta u = u - u_0$ .

$$\delta \dot{x} = f_{x_0} \delta x + f_{u_0} \delta u \quad (5)$$

Then, the application of the methods of linear control theory yields the perturbation control law (6).

$$\delta u = K\delta x \quad (6)$$

Since the coefficients in (5) depend on the nominal trajectory, the process must be repeated for sufficiently large number of nominal trajectories  $(\dot{x}_0, x_0) \in F$  until  $F$  is adequately covered. The result is a scheduled gain matrix  $K(\dot{x}_0, x_0)$ , and the complete control law is

$$u = g(\dot{x}_0, x_0) + K(\dot{x}_0, x_0)(x - x_0) \quad (7)$$

The major drawback of this approach is that when the state equation (1) is highly nonlinear, the procedure for choosing the proper set of nominal trajectories to cover the flight envelope  $F$  is, at present, rather unclear. For this reason we at Ames have decided to investigate a different approach.

Consider the trim equation (4). Suppose that initially  $x = x_0$ . Then in the absence of modeling errors the control  $u_0$  will maintain  $x = x_0$ . The tracking will be perfect even if at some point the acceleration of the nominal trajectory is perturbed from  $\dot{x}_0$  to  $\dot{x}_0 + \delta\dot{x}_0$ , provided that  $(\dot{x}_0 + \delta\dot{x}_0, x) \in F$ . The corresponding control is

$$u = g(\dot{x}_0 + \delta\dot{x}_0, x) \quad (8)$$

Now, suppose that initially  $x - x_0 = \delta x \neq 0$ , but that the error can be removed by means of a flyable trajectory. Then there is a perturbed nominal acceleration  $\dot{x}_0 + \delta\dot{x}_0$  which will take  $x$  into  $x_0$  by means of the control law (8). That is, the feedback for the control of process uncertainties can be closed through the trimmap as in equation (8), rather than after the trimmap as in equation (7). Such control by means of continual adjustments in commanded acceleration forms the basis of the Ames approach. The emphasis is shifted from perturbation models on  $F$  to flyable perturbations in commanded acceleration. The next section describes the resulting structure of the control system.

#### FULL FLIGHT ENVELOPE AUTOPILOT

The proposed structure of the autopilot is shown in figure 5. The plant represents the basic aircraft together with attitude and throttle servosystems, and sensors. Everything to the left is the autopilot. It consists of four blocks - trimmap, wind filter, compensator, and command generator - which carry out the following functions.

Trimmap computes the active control  $u_c$  to generate acceleration with inertial coordinates  $\dot{V}_{Sj}$ . For the case shown, the active controls are the commanded attitude and nozzle angle; while the redundant controls are the throttle and flap. Any other partition of the controls is treated similarly. The total commanded aerodynamic force  $F_{SC}$  is transformed into estimated stability coordinates  $F_{VC}$  from which commanded roll  $\phi_V$ , angle of attack  $\alpha_c$ , sideslip angle  $\beta_c$ ,

and nozzle angle  $\nu_c$  are computed online using the nonlinear inverse function  $g$ . The commanded attitude direction cosine matrix is given by

$$A_{cs} = E_2(\alpha_c)E_3^t(\beta_c)E_1(\phi_v)E_2(\gamma_v)E_3(\psi_v) \quad (9)$$

The attitude control system (servo) may operate directly on  $A_{cs}$ . In case Euler angles are required, they are given by  $A_{cs} = E_1(\phi_c)E_2(\theta_c)E_3(\psi_c)$ . In any case, commanded attitude and nozzle are defined.

Wind filter computes smoothed inertial coordinates  $v_g^*$  of aircraft velocity relative to the airmass from body mounted air velocity sensors, and inertial velocity and attitude of the aircraft. The relative velocity is needed in the trimmap to locate stability axes and to convert forces into coefficients. Note that only inertial coordinates of wind are filtered. The aircraft velocity is unaffected. Hence, in the absence of sensor errors and wind,  $v_g^* = V_g$ .

Trimmap, wind filter, and attitude and throttle control systems form an acceleration controller. The input is  $\dot{V}_{si}$ ; the output is the actual acceleration  $\dot{V}_s$  of the aircraft. Moreover,

$$\dot{V}_s = \dot{V}_{si} + e \quad (10)$$

where the error  $e$  depends on the inaccuracies of inversion  $g$  and wind estimates, the presence of unsteady aerodynamics in  $f$  such as  $\alpha$  dot effects, and on the attitude and throttle servo dynamics. It is the purpose of the compensator to generate corrective accelerations  $\dot{V}_{sm}$  to compensate for the error  $e$  of the acceleration controller. Inertial coordinates of position, velocity, and acceleration are transformed into approximately longitudinal, lateral, and normal errors by means of the direction cosine matrix  $A_{vc}$  computed from the commanded inertial velocity  $V_{sc}$ ; the errors are weighted by constant gain matrices  $K_1$ ,  $K_2$ , and  $K_3$  commensurate with the acceleration capacities of the aircraft in these directions, and the result is filtered to insure compatibility with attitude and throttle servo dynamics. The corrective acceleration is transformed back into inertial space and added to the command  $\dot{V}_{sc}$  to give the input  $\dot{V}_{si}$ . In this way, the feedback is closed around the process uncertainties  $e$  so that the representation

$$\dot{V}_s = \dot{V}_{sc} \quad (11)$$

is sufficiently accurate provided that  $\dot{V}_{sc}$  is admissible, namely  $(\dot{V}_{sc}, V_s)$  is flyable and the bandwidth of  $\dot{V}_{sc}$  is suitable restricted.

The last major block of the autopilot is the command generator. Its purpose is to provide only admissible commands to the acceleration controller. One of the subblocks defines the autopilot mode. For the case shown in the diagram, 27 modes are available. Every mode defines whether position, velocity or acceleration is to be tracked in each of the three axes. Thus, mode (0,0,0) requests three axis acceleration tracking; mode (1,1,1) requests three axis velocity tracking; etc. As an example of the use of modes suppose that the autopilot is in mode (2,2,2) tracking position of a 4-D trajectory commanded by the air traffic control (ATC) as the aircraft penetrates a heavy, localized turbulence. The mode may have to be changed to, say, (1,1,1) or possibly even (0,0,0). On exiting the turbulence, the mode may be returned

back to (2,2,2). The command generator must generate an admissible trajectory for bringing the aircraft back on the trajectory commanded by the ATC.

The ATC trajectory may be transmitted continuously to the aircraft, or more likely, it may be generated onboard from a given set of trajectory parameters. The latter may be transmitted by the ATC or selected by the pilot. In any case, if the commanded trajectory  $(R_{sc}^*, V_{sc}^*, \dot{V}_{sc}^*)$  is discontinuous in any of the variables (e.g. "step down altitude by 500 feet" or "change glide path from  $-7.5^\circ$  to  $-2^\circ$ "), the command generator must generate the required flare maneuver.

Such flare maneuvers are generated by means of transition dynamics. This subblock consists of a stable state equation, initial conditions, and an output map. At the time of the initiation of the transition dynamics,  $(R_{sc}, V_{sc}, \dot{V}_{sc}) = (R_s, V_s, \dot{V}_s)$ . At the end of the transient,  $(R_{sc}, V_{sc}, \dot{V}_{sc}) = (R_{sc}^*, V_{sc}^*, \dot{V}_{sc}^*)$ . The dynamics of the transient are made compatible with the acceleration controller by a proper selection of the state equation. To ensure continuity in position, velocity, and acceleration, the state equation must be at least three-dimensional (and three-axis). In the diagram, a linear state equation is shown. Nonlinear transition dynamics are currently being designed to permit arbitrarily large initial deviations from the ATC command.

The feasibility of the autopilot has been tested by application to the unmodified C8A and the Augmentor Wing Research Aircraft for which detailed simulations are available at Ames. Present indications are that the proposed structure is feasible, although final evaluation must await flight tests which are scheduled in 1976.

The present paper presented an overview of the proposed design methodology. Several reports, currently in preparation and soon to appear, discuss the methodology in greater detail.

## CONCLUSION

The proposed design approach has several advantages, among which are the following.

- (1) The approach is applicable to a large class of aircraft with nonlinear dynamics.
- (2) The approach is nearly algorithmic.
- (3) The approach is invariant for a wide spectrum of tracking accuracy requirements.
- (4) There is an effective trade-off between tracking accuracy requirements and computer requirements and a priori knowledge of system dynamics.

Present indications are that the proposed design methodology is feasible, but definite evaluation must await flight tests.

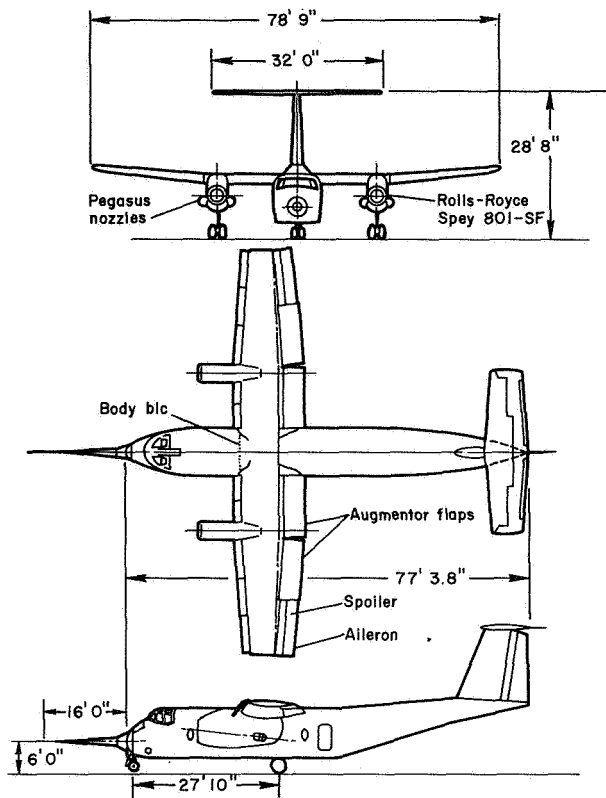


Figure 1. Modified C-8A, General Arrangement

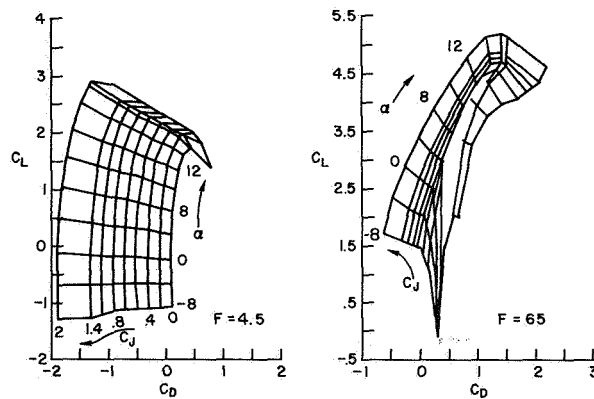


Figure 2. Typical Wing-Body Polars of the Augmentor Wing

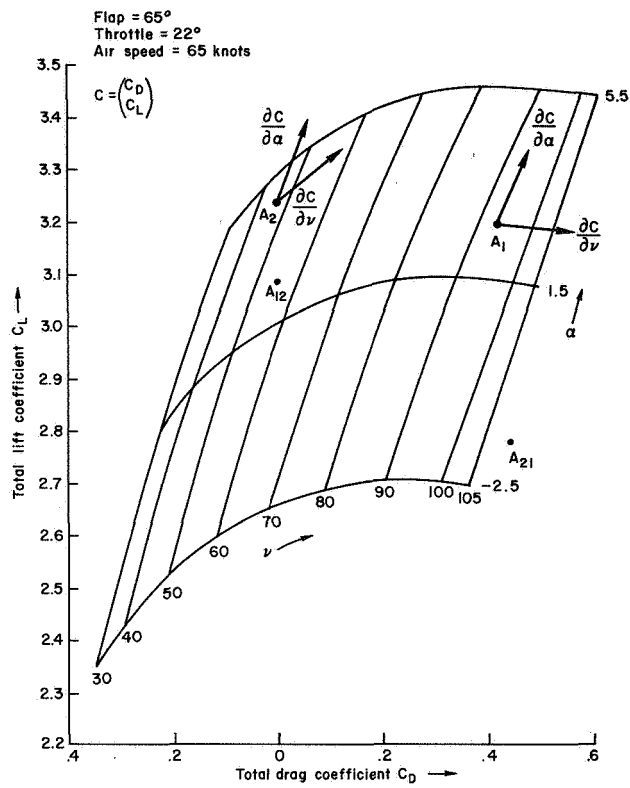


Figure 3. Total Force Coefficient

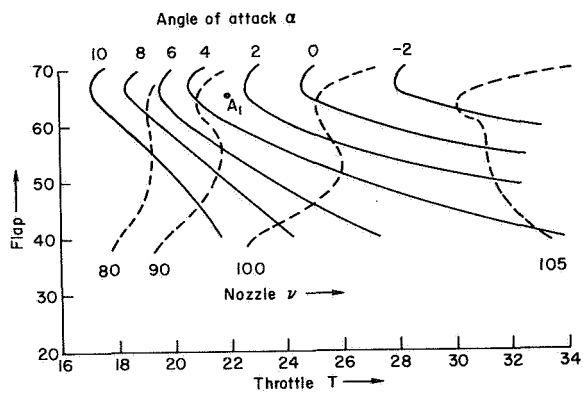
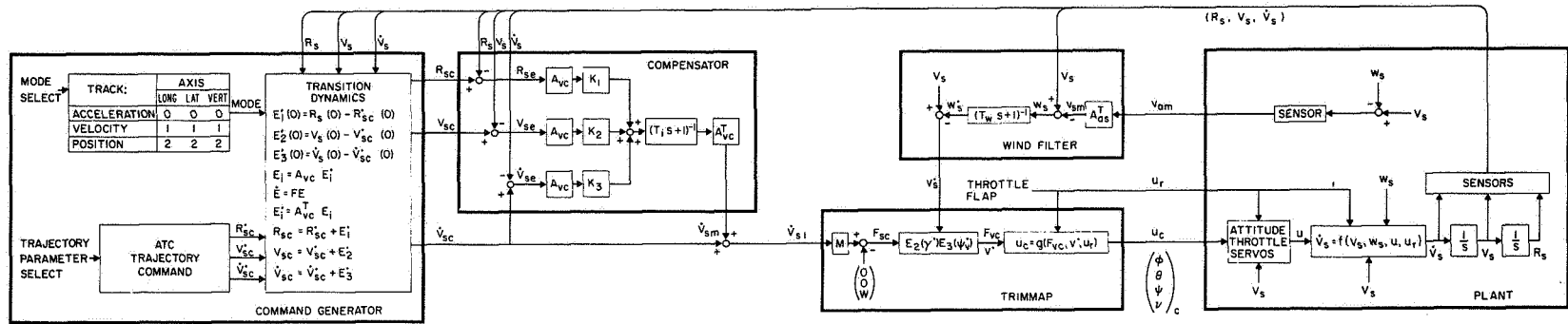


Figure 4. Controls for One Value of Total Force Coefficient





- $(R_s, V_s, \dot{V}_s)$  INERTIAL COORDINATES OF AIRCRAFT POSITION, VELOCITY, ACCELERATION  
 $(R_{sc}, V_{sc}, \dot{V}_{sc})$  INERTIAL COORDINATES OF ATC POSITION, VELOCITY, ACCELERATION  
 $(E_1, E_2, E_3)$  INERTIAL COORDINATES OF TRANSITION POSITION, VELOCITY, ACCELERATION  
 $(R_{sc}, V_{sc}, \dot{V}_{sc})$  INERTIAL COORDINATES OF COMMANDED POSITION, VELOCITY, ACCELERATION  
 $(R_{se}, V_{se}, \dot{V}_{se})$  INERTIAL COORDINATES OF ERROR POSITION, VELOCITY, ACCELERATION  
 $A_{vc}$  DIRECTION COSINE MATRIX OF COMMANDED HEADING  
 $K_1$  LONGITUDINAL, LATERAL, VERTICAL POSITION ERROR GAIN MATRIX  
 $K_2$  LONGITUDINAL, LATERAL, VERTICAL VELOCITY ERROR GAIN MATRIX  
 $K_3$  LONGITUDINAL, LATERAL, VERTICAL ACCELERATION ERROR GAIN MATRIX  
 $T_1$  TIME CONSTANT OF STABILIZING FILTER  
 $\dot{V}_{sm}$  INERTIAL COORDINATES OF CORRECTIVE ACCELERATION  
 $\dot{V}_{s1}$  INERTIAL COORDINATES OF TOTAL ACCELERATION COMMAND

- $M, W$  AIRCRAFT MASS, WEIGHT  
 $F_{sc}$  INITIAL COORDINATES OF COMMANDED AERO-FORCE  
 $F_{vc}$  STABILITY COORDINATES OF COMMANDED AERO-FORCE  
 $E_2(\gamma^*) E_3(\psi^*)$  DIRECTION COSINE MATRIX OF STABILITY AXES  
 $v^*$  FILTERED AIRSPEED  
 $V_{om}$  BODY COORDINATES OF MEASURED AIR VELOCITY  
 $w_s$  INERTIAL COORDINATES OF WIND  
 $V_{sm}$  INERTIAL COORDINATES OF MEASURED AIR VELOCITY  
 $w_s^*$  INERTIAL COORDINATES OF FILTERED WIND  
 $v_s^*$  INERTIAL COORDINATES OF FILTERED AIR VELOCITY  
 $A_{os}$  DIRECTION COSINE MATRIX OF BODY AXES =  $E_1(\phi) E_2(\theta) E_3(\psi)$   
 $(\phi, \theta, \psi)$  EULER ANGLES OF BODY AXES

Figure 5. Full Flight Envelope Autopilot